J. Condensed Matter Nucl. Sci. 31 (2020) 20–41

Research Article

Investigations of "Heat after Death"

Analysis of the Factors which Determine the Tardive Thermal Power and HAD Enthalpy

Mitchell R. Swartz*

JET Energy Inc., Wellesley Hills, MA 02481, USA

Abstract

This report closely examines the heat energy generated during the discharge period after cessation of all input electrical power to active CF/LANR components ("Heat after Death" or "HAD" energy). This is potentially a very important source of energy because the techniques shown here, can increase the excess energy gain of CF/LANR reactions by at least 410%. In addition, by monitoring both the calorimetry and the V_{oc}, detailed knowledge of the deuteron distribution and flows within the palladium are revealed. These experiments revealed that initially only one in 2300 deuterons takes part in the desired reactions of HAD excess enthalpy production, for a net utilization of 0.04% of the loaded deuterons at that time. This decreases over time. Integrated over the entire HAD regime, this deuteron participation levels falls, and eventually only 1 in 10^6 deuterons participates in the desired fusion reactions.

Keywords: Heat after death, Heterodyne excess power, Lumped parameter, Lumped component, Phusor®, Phusor®-type component, Tardive thermal power

1. Introduction

1.1. Tardive thermal power and "Heat After Death"

After being successfully driven to excess heat conditions, some cold fusion systems [1–26] continue to produce significant delayed ("tardive") thermal power ("TTP"), even after the input electric power is terminated (Fig. 1). It was first reported by Pons and Fleischmann [5] in a palladium cathode in heavy water after it was electrically driven to an active excess heat-producing state ("cold fusion"). They reported on this new phenomenon calling it "Heat After Death" ("HAD").

*Dr. Mitchell R. Swartz ScD, MD, EE, E-mail: jet@nanortech.com.

The term "death" refers to cessation of the input electrical drive (electrical polarization) power. Aqueous cells containing D_2O were first electrically driven to boiling, and thereafter, when the electrolyte was fully electrolyzed and gone, did not cool down immediately as expected [5–9]. In one of the original HAD experiment reported by Pons and Fleischman, the electrolysis cell had finally run out of heavy water due to the electrolysis, thereby unintentionally and inadvertently creating the condition of no further input electrical power. This is due to the fact that the electrical circuit became "open circuited" and the heavy water system's electrical circuit was cut-off.

The HAD has the units of energy. The rate of appearance ("time derivative") of the heat after death [9–12] is the tardive thermal power. TTP is thus the heterodyne "excess" power which continues to be generated even AFTER after all of the input electrical power is terminated. The word "heterodyne" is used because of the actual the denotation of the word (***). "Hetero" is an English word meaning "other". "Dyne" is the root word of the words dynamite, dynamo and dynamic. "Dyne" comes from the Greek word dunamis ($\delta\nu\alpha\mu\iota\varsigma$) which means 'power' and was derived from the Greek translation of "koach"(כח), the Hebrew word used in the Bible to describe the miraculous deliverance of Israel at the Sea of Reeds (Exodus 15.6). Thus, with the correct denotation, tardive thermal power is the heterodyne response of an active Pd/D_2O cold fusion/LANR cell which is correctly electrically driven at its optimal operating point, with adequate phonons, and in the absence of quenching materials. (***) The popular use of heterodyne ("connotation") is that it describes the phenomenon of a non-linear system changing of the frequency of two incoming radio signals or photons. The two are transformed to now four with the heterodyne action adding to the original two, the sum of, and difference between, the two signals (photons). In 1901, Canadian Reginald Fessenden coined the word "heterodyne", when he invented and demonstrated his direct-conversion heterodyne receiver which made telegraphy signals audible. His unstable local oscillator ("LO") was perfected in 1918, by American engineer Edwin Armstrong. Armstrong's superheterodyne used a variable LO to move radio frequency signals, by dial, to the audio range making demodulation and broadcast radio possible. Nonetheless, this word "heterodyne" actually is quite precise and appropriate for HAD because it describes "power" in its denotation.

1.2. Studies of the "Heat After Death" phenomenon

Pons and Fleischmann's (FP's) heat after death enthalpies were reported in the range of 302–3240 J, with peak HAD excess power of 0.8 W (8 W/cm^3). They described several possible HAD scenarios including those where the electrolyte solution remains or is lost, and whether boiling is achieved, along with other conditions.

Since then, HAD has been confirmed by Miles et al. [6,7], Mizuno [8] and Swartz and Verner [9–12]. Mizuno reported HAD which yielded 1.2×10^7 J over 10 days in 1991. Mengoli used an FP cell, and after five days of electrical drive, the cell is reported to have continued with HAD for 27.3 h, initially at 0.82 W.

Swartz and Verner [9–12] reported at ICCF10, and thereafter, that TTP information was resolvable using high impedance Phusor® -type LANR devices with "Dual ohmic control calorimeters" after they were loaded, activated, and driven at their OOP [9], and analyzed for their kinetics [10–12].

1.3. Tardive thermal power

The advantages of studying TTP are many. First, the most important advantage is that this may be one of the most electrically noise-free operational modes in which to examine the materials. During this mode of operation there is no synchronous interfering input electrical power and resultant noise. Therefore, one is able to more closely examine the time course of the rate of heat energy (HAD) generated during this discharge period, long after cessation of all input electrical power. HAD excess heat production was measured from active devices after they were initially loaded and driven for several hours.

The second advantage is that understanding this region of operation has led to maximizing the output of these systems by at least 410% (*vide infra*).

A third advantage is that "lumped component" (also called "lumped parameter") models can be used to analyze the kinetics. The kinetics reveals HAD has more than one evanescent heat generating site [10–12] and instead multiple sites contribute to the observed TTP. HAD fall off is characterized by one site (or group of sites) with a time constant of several minutes, and a second site having a longer time constant of ∼20 minutes to hours. This is consistent with their being vicinal surfaces and deeper sites in the volume, with the longer time constant secondary to the deeper location within the lattice. It could also be due to shallow and deeper traps. As a result, in 2005, we suggested a two-site TTP reaction system in the palladium heavy water Phusor®-type system. This was felt to be consistent with both the deep, and the more superficial sites, perhaps up at least to ∼40–100 μm from the surface. This plurality of sites was previously suggested by both our data, and independent, codeposition results [10–12]. Later, we added a third region to the model at ICCF-14 to account for all the involved loaded layers, from the most superficial from codeposition to the range of deeper sites [12[. This paper begins with a review of those findings, and continues with other significant discoveries from those investigations.

2. Experimental

2.1. Overview

For these HAD investigations, paired joule (thermal) controls and power integration enabled TTP/HAD calorimetry with semiquantitative corrections for both cooling and deuteron-deloading. We then investigated the magnitude of heat production, including with electric discharge spectroscopy. A "lumped component" (also call a "lumped parameter") model was used to analyze HAD not as energy only, but by using the tardive thermal power as a function of time.

2.2. Materials

These experiments used materials and procedures discussed in detail elsewhere [13–20]. The solutions were comprised of a very low electrical conductivity heavy water (deuterium oxide, low paramagnetic, 99.99%, Cambridge Isotope Laboratories, Andover, MA) to minimize the unwanted reactions of electrolysis. The volume of the heavy water solution ranged from 30 to 40 cm^3. The cells are not open to the atmosphere, and efforts are made to keep ordinary water out of them, and to minimize any possible contamination, as we previously reported [13–19]. The anodes were platinum (99.998% metals basis, Alfa Aesar). The cathodes were palladium (99.98+% metals basis, Alfa Aesar).

2.3. PHUSOR®-type system

Figure 1 is a schematic which shows all three bottles, the electrodes, the ohmic controls, and just a small portion of the diagnostics and temperature probes. The anodes had an active metallic area of 3 cm^2, and a volume of 0.077 cm^3. The cathodes were PHUSOR®-type. Previously, we reported [14,19] on excess heat obtained from PHUSOR®-type spiral-wound palladium cathodes (cathode volume ∼0.5 cm^3) immersed in very low electrical conductivity D_2O with no additional electrolyte, electrically polarized against a platinum anode. These devices can yield significant excess heat (peak excess power production circa 1.5 W, peak electrical power gain of ∼2.7). Here, these types of systems are examined even more closely after termination of the applied electrical power. The PHUSOR®-type cathode consists of a spiral wound wire electrode with an area of 6.7 cm^2. The 12 turns of palladium wire created an active volume of palladium of 0.17 cm^3. The enclosed volume subtended ranged from 1.6 to 58 cm^3.

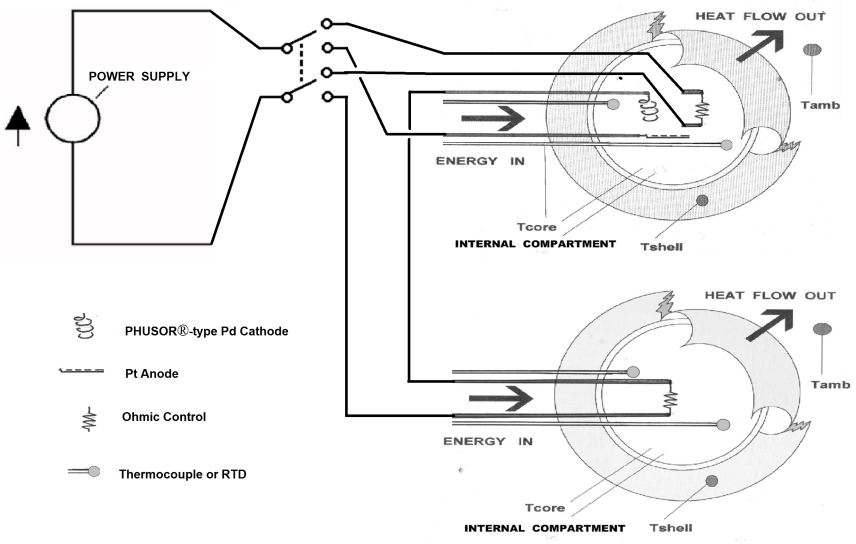

Figure 1. Schematic of setup – calorimetric Setup. (*Top*) Electrical configuration – In this configuration, the electrical power source is alternatively sent to the ohmic control in the first container, or to the CF/LANR cell in the same chamber which is in electrical series with the second ohmic control in the second container. The actual dimensions, positions, the range of diagnostics, and the partially adiabatic barrier are shown schematically, for simplicity. (*Bottom*) The partially adiabatic barrier channeled enabled the "heat flow out" shown in the Electrical configuration to be directed to one of the pair stirling engines [19].

2.4. Calorimetric setup

The calorimetric setup used identical paired polypropylene reactor containers, and a third with no electrical connections as a local thermal control. Each identical container held 30–40 ml of heavy water, and were contained within a second, partially adiabatic, chamber [13–19]. The first container holds the CF/LANR system with the two electrodes, a palladium cathode and a platinum anode, and an internal ohmic control. The second container holds only an ohmic control. The second container was either driven alternatively with the first container holding the CF/LANR cell, or was driven in electrical series with the first cell. Normal cool-off effects of both the PHUSOR®-containing calorimeter and its control are eliminated by subtracting the cool-off of the paired control.

The third container, the internal background control, is not electrically connected to anything. It is a thermal ballast (an additional control of the local average background temperature) and has no internal components, except for its external temperature sensors.

Several types of calibration were used. First, we use thermal (joule) electrical ohmic controls to calibrate the system for semiquantitative accurate calorimetry. The ohmic controls are absolutely needed because calculations by brute force are likely to be quite inaccurate, as has been shown in several flow calorimetry experiments, repeatedly.

In addition, to correct for normal prosaic cool-off, in this system there were TWO ohmic controls, one in each of the paired containers constituting the calorimeter. One ohmic control is used in the main reaction vessel, containing the heavy water and the palladium cathode, to calibrate that cell. A separate ohmic control was also used in the second cell. That ohmic resistor (typically 98.6 kΩ but matched as well as possible to the working impedance of the active cell) is immersed in the identical second container.

2.5. Electrical drive

The electrodes, and control in electrical series, were electrically polarized. This causes a variety of conduction and polarization reactions including loading of the cathode with deuterons. The electrical series arrangement of the paired matched containers in this calorimeter were used as the thermal cool-off (and heat-up) control to correct for possible time-variant changes in thermal heat leakage to the environment, if any, which might occur during the experiment (as has been brought up by Dr. Shanahan, and has been corrected here for years [13–16,18,19]. In that configuration, when the CF/LANR cell is driven to examine its active mode, the electrodes are in electrical series with the joule (ohmic) control immersed in the second container, which is also used during the HAD-measurement run (Fig. 1). This arrangement can semiquantitatively correct for those possible time-variant differences in heat flow loss. Driving was usually at voltages below 150 V, by an electrical current source (Norton equivalent). Either when full loading is achieved, or when an electric potential of ∼125–1500+ V is needed, we used an electrical voltage source (Thevenin equivalent). All electrical input power was terminated when the HAD regime was monitored by V_{oc} and calorimetry.

Electrical currents were derived from electrical current sources (Keithley 225), and were also measured to confirm the outputs (±1% accuracy). Electrical voltage sources included the LAMBDA 340A, HP/Harrison 6525A, and the JET Energy 10K control unit. Electrical potentials were measured with high performance units (±0.5% accuracy, Keithley 610C Electrometer, Keithley 160B, Dana Electronics 5900, Fluke 8350A, and HP 3455A, 5334A and 3490A voltmeters).

The actual applied electric field DOES partially penetrate the cathode as we can measure the voltage across the cathode, and it has a very small resistance which is not zero [26[. As reported, in very high impedance systems, using 4-terminal measurements experiments with anodic platinum plates (0.001–20 mA; 99.7 V, with solution impedances of circa 254 kΩ; excess power of ∼175%) determined the cathode palladium coil (1 mm diameter) to have an impedance of circa 50 mΩ. This intracathodic E-field [26] has led to the discovery that there may even be quasiparticles and quasi-collective particles existing within the cathode, and whose behavior changes just prior to the appearance of excess heat.

2.6. Temperature measurement

Data acquisition is achieved by an Omega OMB-DaqTemp (Omega Technologies; 16 bit resolution, 200 kHz maximum sampling rate, voltage accuracy and precision of $0.015^{\pm 0.005}$ V, temperature accuracy ~ 0.6°C (the lower number is the accuracy, the superscript number is the precision). We use multiple temperature probes and heat flow measurements. Temperature measurements are made by several groups of thermocouples (accuracy of ± 0.8 K).

Generally there are at least two probes at the core. However, for a high temperature measurements ($>$125°C) or when we fear possible quenching contamination the probes are taken to the outside of most inner vessel, and the notions are given that this may be a lower limit to the temperature of the inner container (and derived putative excess heat).

To avoid sampling errors, samples are taken at rates of at least 10 Hz. The noise of the system is mainly quantization and thermal noise and ranges from 1 μW to $\sim$ 10 mW [14,19]. The power gain and excess energy are determined from the differences in temperature between the heavy water cell and background.

2.7. Recombination issues are moot

Recombination issues are moot both experimentally and analytically, and it can not be the origin of these observations for several reasons. First, recombination is not relevant in these experiments because these high impedance aqueous cells were electrically driven at levels below the voltage where any significant amount of heavy hydrogen gas (D_2) was generated. This was done to minimize gas evolution – and therefore possible recombination – the CF/LANR cells, as has been taught in the author's papers since 1990s.

Second, recombination is not a factor because the electrical input is defined as $V \times I$, and the thermoneutral potential is not subtracted in any derivation. The reason that the thermoneutral potential is not subtracted in determining the power gain is because that it is in the denominator of the incremental power gain factor, and any subtraction can, and does, lead to a false positive or false magnification of the actual excess incremental power gain, if any.

Third, as reported below, we have discovered that the XSH HAD result is shown to be dependent on the magnitude of the previously applied driving voltage. This would not be present and occur this way, if this was just recombination.

2.8. Methods

2.8.1. *Calorimetry data analysis*

The calorimetry curves shown are derived using carefully calibrated techniques. The reader is referred back to the key papers where the two pole calorimetry, augmented by heat flow measurements, is discussed, and for space they have not been reconsidered here. This system was used at ICCF10 in the open demonstration and at many thereafter, as reported [1,9,13–15], where the methods of calorimetry were discussed.

The exact setup used to derive the excess heat results before the "HAD" region, the exact calculations of input and output power, and how the incremental power gain and excess energy are determined have been discussed in the previous papers [9,13–16, 18,19].

In these measurements, time integration of the electrical input power and output thermal power are each used to generate total energies, both input and output. Therefore, the binding energies associated with deuteron loading into the palladium, and that associated with phase changes if any, are also measured and can be resolved and considered, too.

2.8.2. *Lumped component analysis*

In actuality, the physics of cold fusion involves material and energy flow in a very inhomogeneous stereoconstellation of parts ("system" which becomes even more inhomogeneous on the application of the applied electric field intensity. A "lumped component" (also call a "lumped parameter") model was used to analyze HAD, examining the tardive thermal power and $V_{\rm oc}$ as a function of time (Sections 5.1–5.6). This lumped parameter model simplifies this analysis by considering how the system appears when visualized as a two-wire 'lumped component' model. Thus, it involves the notion of two resistive, and a capacitive (storage), components.

These are first order simplifications that enable further analysis. In fact, by examining the temporal changes, lumped component electrical analysis clarifies the excess heat production which continues for several hours after cessation of input electrical power to an active loaded spiral-wound palladium cathode/D_2O/platinum anode system.

3. Results

3.1. Post-electrical TTP measurements

The PHUSOR®-type CF/LANR components were initially loaded and driven for several hours and more, during the active phase. After the devices were driven, determination of the possible heat after death was made by semiquantitative analysis with semiquantitative correction for (a) the joule (thermal) ohmic controls, (b) the deloading (followed through $V_{\rm oc}$), and (c) the normal cooling by the paired system.

After accounting for other sources of energy, including Poiynting vector, prosaic energy storage and release, and D loading and deloading energies, D_2 and O_2 recombination, and possible phase changes, it is clear that HAD does exist for Pd, at least under these conditions (Figs. 2A,B and 3A,B). These figures show the results of four experiments producing HAD. They show TTP and its integrated $E_{\rm HAD}$. Shown in Figs. 2A,B and 3B are the excess enthalpies observed during electrical activation, and after disconnection of the electrical drive (the "HAD regime"). There is significant continued emission of excess heat, long after the termination of all electric input power. Figure 3B shows the heating of a second volume of water using the HAD from the previously active cell in its heterodyne TTP-producing mode.

Figure 2A shows the calorimetry of a PHUSOR®-type Pd/D_2O/Pt cell and its joule control during both the active state and during the HAD region. It shows the input electrical powers and observed output thermal powers (and energies).

There are eight curves. Four involve power and four others involve energy. They present the input electrical powers and observed output thermal powers (and energies) for a Pd/D_2O/Pt cell and the joule control as a function of time Eight curves are shown; four involve power; four involve energy. In Fig. 2A, the input and output powers are linear. The HAD instantaneous power (tardive thermal power) is marked.

It can be seen that the observed output thermal power is much greater compared to the electrical input power for the deuteron-loaded system, as compared to the joule control. With an initial drive potential of ~300 V to 330 V) for several hours, the Pd phusor system produced an initial peak tardive thermal power of 1.3 W (~7.7 W/cm^3 [9]). The integrated HAD excess enthalpy was 5200 J, and the time constant of the falloff was ~70 min. The time was determined by curve fitting on the computer and by using exponential approximations which make the slope linear on a log time axis. Examples are shown in Figs. 4A,B and 5.

It can also be seen that for the ohmic joule (thermal) control that the integrated energies of the input and output rise with parallel slopes. By contrast, in the deuterium-loaded heavy water systems, there is a gap increasing over time, corroborating that there has been active heat generated.

The curves in Fig. 2A confirm, both by the difference between the control and observed excess power and the differential in excess energy by slope, there is excess heat output; and by the calorimeter-matched calorimetry, there is

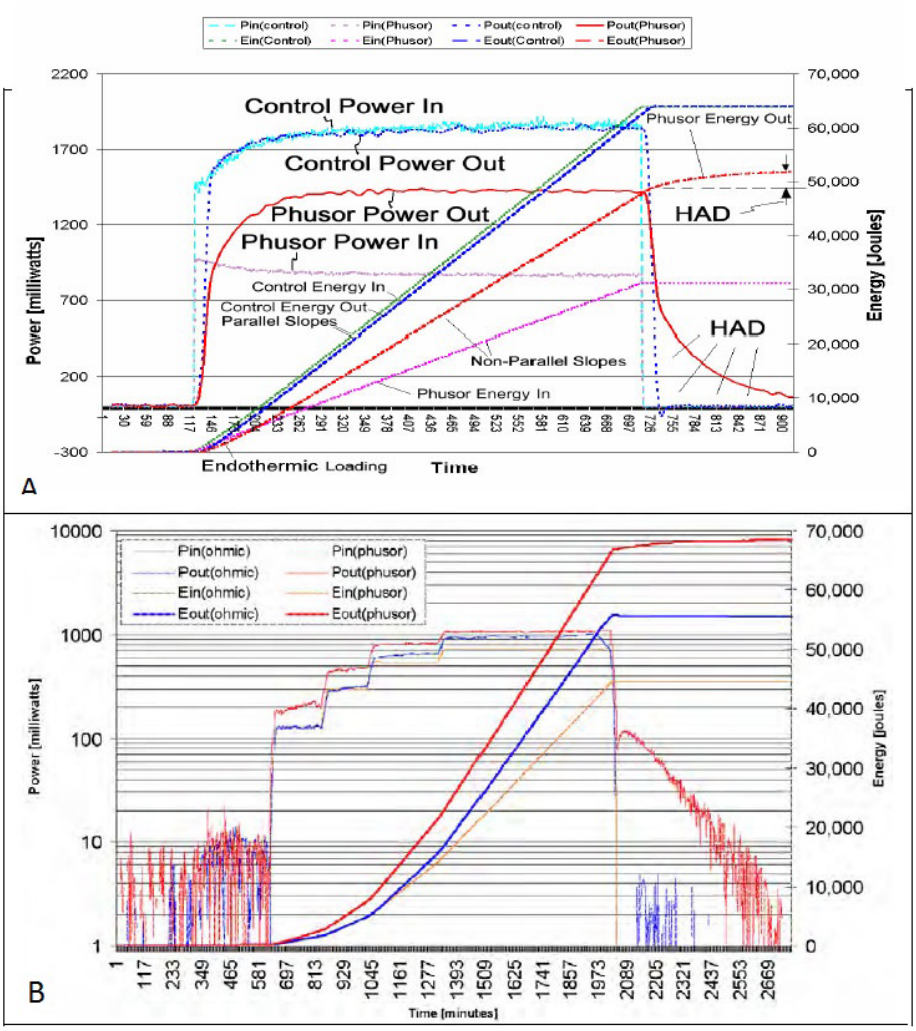

Figure 2. Calorimetry of PHUSOR®-type Pd/D_2O/Pt cells and their joule controls, showing the input electrical powers and observed output thermal powers (and energies). (A) (*top*) – Input electrical powers and observed output thermal powers (and energies) for a PHUSOR®-type Pd/D_2O/Pt cell and the joule control as a function of time. (B) (*bottom*) – Input electrical powers and observed output thermal powers (and energies) for both the heavy water PHUSOR®-type Pd/D_2O/Pt cell and the joule control as a function of time.

HAD output of this deuterium-loaded system.

Figure 2B shows the calorimetry of a PHUSOR®-type Pd/D_2O/Pt cell and its joule control during both the active state and during the HAD region. This figure, of a different run, has the input and output powers plotted on logarithmic axes so that the background noise of the system before, during the electrical drive, and after the electrical drive is finished, are clearly shown. It shows the input electrical powers and observed output thermal powers (and energies) in eight curves.

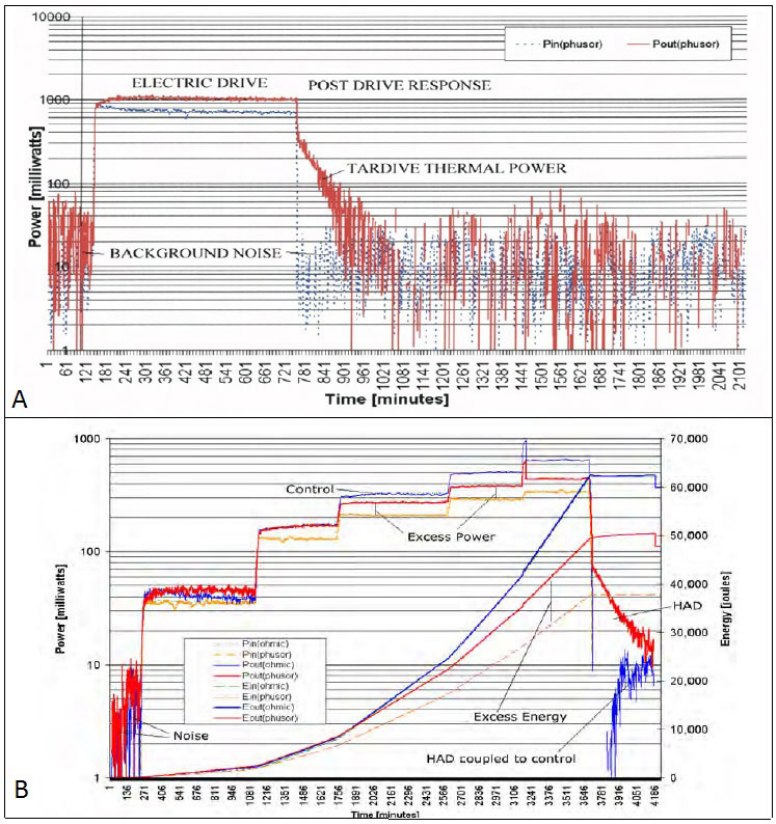

Figure 3. Calorimetry of PHUSOR®-type Pd/D_2O/Pt cells and control. (A) (*top*): Input electrical powers and observed output thermal powers as a function of time for a heavy water PHUSOR®-type Pd/D_2O/Pt cell and the joule control as a function of time. The background noise levels can be seen. (B) (*bottom*): Input electrical powers and observed output thermal powers as a function of time for a heavy water PHUSOR®-type Pd/D_2O/Pt cell and the joule control as a function of time. The background noise levels can be seen, and here they show transfer of the HAD energy to the control container which is heated (labeled HAD coupled to control)], further proving the existence of HAD.

Figure 2B shows the results of a run with a incremental excess power gain of 1.98, and peak output power of 1.1 W. The incremental excess power was 366 mW. There was an integrated excess heat of 153% beyond the input energy, which was 23,613 J. The energy obtained during HAD was 3610 J.

The active cell was driven at four levels with V_{applied} ranging from 100 to 230 V. The loading energy was 22 J. At the end of the active drive state, V_{oc} was 2.0 V, suggestively heralding the excess heat indirectly, as we reported at ICCF-10 [14–16].

It can be seen that for the ohmic joule (thermal) control that the integrated energies of the input and output rise with parallel slopes, and they overlap. By contrast, in the deuterium-loaded heavy water systems, there is a gap which increases over time, corroborating that there has been generated excess heat.

The curves in Fig. 2B confirm, both by the difference between the control and observed excess power and the differential in excess energy by slope, there is excess heat output; and by the calorimeter-matched calorimetry, there is HAD output of this deuterium-loaded system.

Figure 3A shows the calorimetry of a PHUSOR®-type Pd/D_2O/Pt cell and its joule control during both the active state and during the HAD region. In this case, they had a slightly different adiabatic shell and is designed as a 6000Neo1-modified PHUSOR®-type system. The "Neo" refers to the neoprene isolation chamber used in the system.

This figure, of an additional different run, has the input and output powers plotted on logarithmic axes so that the background noise of the system before, during the electrical drive, and after the electrical drive is finished, are clearly shown.

Figure 3A shows the results of a run with a incremental excess power gain of 2.23 (223% beyond the input electrical power), and peak output power of 1.26 W. The incremental excess power was 293 mW. The integrated excess energy was144% beyond the input which was 11,839 J. The energy obtained during HAD was 1558 J. V_{applied} was 600 V. The curves in Fig. 3A confirm by the difference between the control and observed excess power, there is excess heat output; and by the calorimeter-matched calorimetry, there is HAD output of this deuterium-loaded system.

Figure 3B is very important. It presents the very first time tardive thermal power (the time derivative of HAD energy) was used to heat another volume of water. This transfer of energy from HAD to a second volume is shown clearly, further proving the existence of HAD. This region is labeled ("HAD coupled to control"). Figure 3B shows the calorimetry of a PHUSOR®-type Pd/D_2O/Pt cell and its joule control during both the active state and during the HAD region. Presented are the input electrical powers and observed output thermal powers as a function of time for a PHUSOR® -type Pd/D_2O system over a four day run. Shown in Fig. 3B are four power curves, and four energy curves, but because two overlap so well, only three are easily observed. This figure, of a very different run, has the input and output powers plotted on logarithmic axes so that, again, the background noise of the system before, during the electrical drive, and after the electrical drive is finished, are clearly shown.

Figure 3B shows the results of a run with a incremental excess power gain of 1.70, and peak output power of 460 mW. The incremental excess power was 140 mW. There was an integrated excess heat of 134% beyond the input energy, which was 12,681 J. The energy obtained during HAD was 1011 J. The loading energy was 8 J. The system shown in Fig. 3B was driven at five levels with V_{applied} ranging from 50, 100, 130, 155, to 170 V. V_{oc} ranged from 1.7 to 2.1 V, consistent with excess heat.

It can be seen that for the ohmic joule (thermal) control that the integrated energies of the input and output rise with parallel slopes, and they overlap. By contrast, in the deuterium-loaded heavy water systems, there is a gap which increases over time, corroborating that there has been generated excess heat.

There is significant transfer of energy to the ohmic control volume as demonstrated convincingly by the rising in its thermal background (labeled where the background rises from circa 2 mW to circa 10 mW equivalent background power).

Therefore, the curves in Fig. 3B confirm, both by the difference between the control and observed excess power and the differential in excess energy by slope, there is excess heat output; and by the calorimeter-matched calorimetry and by the transfer of heat to the control compartment, there is HAD output of this deuterium-loaded system.

Furthermore, the existence of energy (heat) transfer to the second container proves conclusively that this is no ordinary cool-off, but that excess energy continues to be made by the CF/LANR system – even after cutoff of the applied electric field intensity.

3.2. Determination of time constants from decay rates

Time constants are observed in both the measured "excess" enthalpy after disconnection of the electrical driving source, and also in the V_{oc} (observed by "electric discharge spectroscopy") also during that period. The decline in excess heat and the V_{oc} are presumably be related to loss of deuterons from the previously fully loaded cathode ("deloading"). In that light, the decline occurs because the lowest energy of the PdD_2 alloy system appears to be at a loading between approximately 0.25 and 0.45.

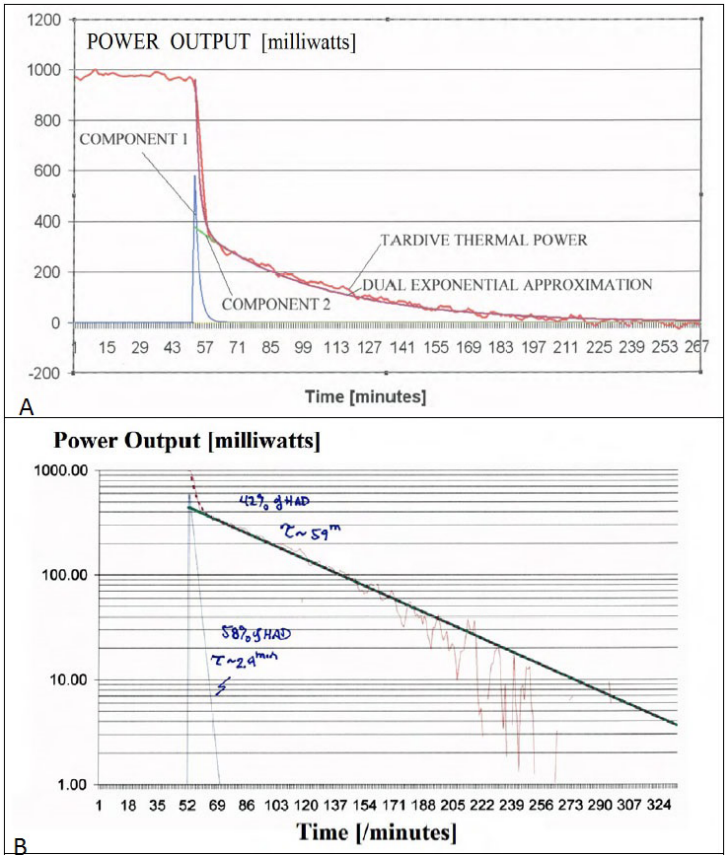

Figure 4. Demonstration of Multiple Time Constants in TTP and V_{OC}. (A) (*top*): TTP discharge spectrum of a Pd/D_2O system (6000Neo1-type PHUSOR®) with a power gain of 2.23, and an incremental integrated excess heat of 1.44%. (B) (*bottom*): TP discharge spectrum of a Pd/D_2O system 6000Neo1-type PHUSOR® with a power gain of 3.66, and an integrated excess heat of 173%.

The time constants were determined by computer fit using standard packages, and is also clearly seen in Figs. 4B and 5 where the horizontal times are arranged to make the exponential fall-off appear as a straight line.

Close examination of the TTP as a function of time shows that there are two, or sometimes, three, time constants involved. The presence of two- and then three-compartment models being required to fit the falloff V_{oc} data of the tardive thermal power was discussed at ICCF14 [21,24]. Whether these are determined by deuterons being in shallow or deep energy traps, or by the deuterons (also) being at disparate locations within the palladium (which they are clearly because there is the codepositional surface and the sites deeper within the loaded Pd) is not clear at the moment. Three examples follow; two demonstrating a 2-compartment model.

Figure 4A shows the TTP discharge spectrum of a Pd/D_2O system (6000Neo1-type PHUSOR® with a power gain of 2.23, and an incremental excess power was 293 mW. The integrated excess heat was 1.44% beyond the input which was 11,839 J. The HAD energy was 1,558 J. The time constants are ~2 and 53 min, using the 2-compartment model. These comprise 60% and 40% of the loaded sites within the palladium respectively.

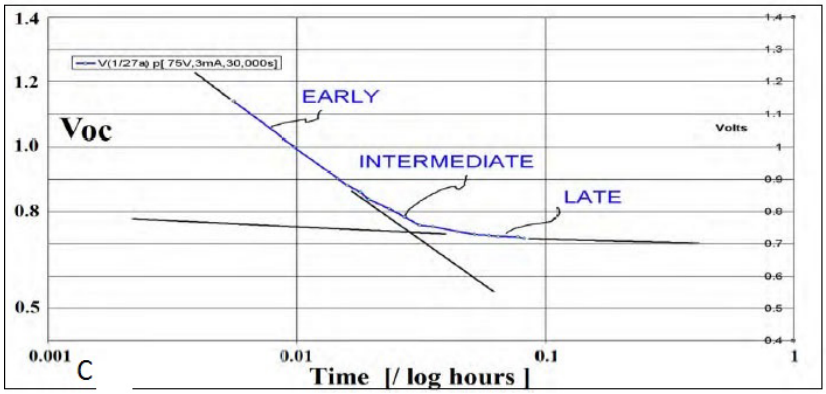

Figure 5. Demonstration of multiple time constants in TTP and V_{oc}. V_{oc} (open circuit) Discharge spectrum of palladium electrode 3-compartment TTP discharge spectrum of a Pd/D_2O system PHUSOR®) with a power gain of, and an integrated excess heat of beyond the input. Three time constants are seen suggesting a possible need for a three-site model. $V_{applied}$ was 75 V, delivering circa 3 mA current for circa 30,000 s.

Figure 4B shows the TTP discharge spectrum of a Pd/D_2O system (6000Neo1-type PHUSOR® with a power gain of 3.66 (366%), and an integrated excess heat of 173% beyond the input which was 10,104 J. The HAD energy was 206 J. The peak output power was 1.26 W. V_{applied} was 600 V. The time constants are ~2.9 and 59 min. The first occupation site (shallow site) constituted about 58% of the palladium.

3.3. Electric discharge spectroscopy

We have reported that electric discharge spectroscopy is extremely useful, and that it offers insight into excess heat and as to whether adequate loading has been achieved for a palladium sample [10–12]. The open circuit voltage (V_{oc} ; remnant voltage after cessation of the electrical input) is the measured electric potential between the deuteron-loaded palladium cathode and the anode of platinum, beginning immediately after the active phase. After charging, if the voltage source (or electric current source) is disconnected, the open circuit voltage (V_{oc}) between the palladium and the anode can be followed as a function of time [10–12]. The post-electrical excess enthalpy can be followed *in situ* by the open-circuit voltage (V_{oc}).

Figures 4A,B and 5 show the examples of electric discharge spectroscopy during the heat after death phenomenon. Shown is the electrical discharge spectrum of a palladium electrode after full loading achieved by driving the system with 75 V, 3 mA, for 30,000 s. The vertical axis is the open circuit voltage, V_{oc}. This electric discharge spectrogram is made by following the V_{oc} while also measuring the excess enthalpy after disconnection of the electrical driving source. There is enough resolution that it is apparent that there are probable three regions of electrical discharge behavior [19,21,24].

The decay rate of all active Pd/D_2O samples studied has been similar, both in time, and in the fact that they appear to consist of at least two, possibly three contributing independent decay rates.

It is not clear why there is linear falloff of the TTP. It may be due to the deloading which is limited by the surface. It may be due to the fact that the heterodyne tardive thermal power strictly follows the V_{oc} which has linear fall off in the early exponential region.

3.4. V_{oc} Can Herald excess heat and HAD

Previously, we reported [10–12] that the post-drive open circuit voltage (V_{oc}) is a useful predictor of excess heat generation, and that there is a threshold potential V_{oc} required for the excess heat generation. A V_{oc} greater than 0.7 V (threshold) is consistent with generated excess heat [14], as follows: Prior to full loading and activation of excess heat, the V_{oc} remains on the order of, or less than, ~0.7 V, and the palladium–platinum system does not demonstrate excess heat. However, if the open circuit voltage (V_{oc}) is ~1.8 to 2.7 V, then excess power is observed. A V_{oc} of 1.9 V corresponds to a system with a reasonable power gain of about 170%. A V_{oc} of 2.4–2.7 V corresponds to a better system with a power gain of about 230% or more.

Given that is a dynamically evanescent exponential falloff, it is necessary to state when it is taken after cut-off of the active state. Here, it is characterized by the 1 min, and it is a useful metric of estimating how the cell/system/electrode has performed with respect to producing excess heat. It is not specific, however, and the excess heat also must be measured by calorimetry and heat flux measurements.

We now report that the post-electrical input "excess" enthalpy can be followed *in situ* by the open-circuit voltage (V_{oc}), as well. Over time, as the TTP decreases, there is a decreasing V_{oc} . The threshold potential V_{oc} required for the excess heat generation during active drive in these devices is the same threshold potential V_{oc} at which the heat after death terminates. V_{oc} at equilibrium ($V_{\mathrm{oc,equilibium}}$) is 0.7 V. When the HAD ceases, the V_{oc} is ~0.7 V.

3.5. Applied previous driving voltage is also predictive

We now report that V_{oc} alone is NOT predictive of the actual magnitude of the HAD excess enthalpy. V_{oc} and the charging voltage, V_{applied} *both* play a role in determining the presence and magnitude of HAD excess enthalpy. TTP is controlled by the prior history of the system, including input electrical power, and if it was driven at its optimal operating point. Figure 5 shows the heterodyne TTP of a PHUSOR®-type Pd/D_2O/Pt cell as a function of V_{oc} and the previous V_{applied} during the active drive mode, for three different experiments. The three runs were driven by three different initial filling ("drive") applied voltages of 115, 200 and 300 V. Attention is directed to the fact that there are three characteristic curves (dependent upon V_{applied}) which each describe the HAD enthalpy as a function of V_{oc} (Fig. 6). The implication is that HAD enthalpy cannot be directly related to only V_{oc} because different characteristic curves are observed when HAD excess enthalpy is plotted as function of V_{oc}.

It can also be seen that the tardive thermal power decreases as V_{oc} falls, and there exists a clear threshold potential of 0.7 V. Previously, we reported that V_{oc} at equilibrium ($V_{\mathrm{oc,equilibium}}$) prior to a cathode showing excess heat is 0.7 V. Now when the rate of change of HAD (TTP) ceases, the V_{oc} is also ~0.7 V. Although these curves look as if the falloff might be in the range and 0.72–0.75 V, it is noted that there is both dispersion on the graph in the x-direction,

Table 1. Observed and Expected HAD excess enthalpies.

V_{applied} (nominal) (V)	V_{applied} (range) (V)	$C_{\mathrm{Pd,D}}$ micromoles/volt †	V_{oc} 1 min ave.	V^*_{oc} (V) ‡	E expected ($C_{\mathrm{Pd,D}} \times V_{\mathrm{applied}} \times V_{\mathrm{oc}}$) (J)	E observed (J)	$\frac{\mathrm{(O-E)}}{\mathrm{O}}$ (%)
115	107-120	64	1.5	0.8	567	700	19%
200	188-201	64	1.5	0.8	987	2,800	65%
300	270-330	64	1.6	0.9	1,665	5,200	68%

†The star (*) is added to remind the reader that the units are voltage, but the value is semiquantitatively corrected with respect to the equilibrium threshold potential ($V_{\mathrm{oc,equil}}$).
‡This is a lower limit because of the averaging process.

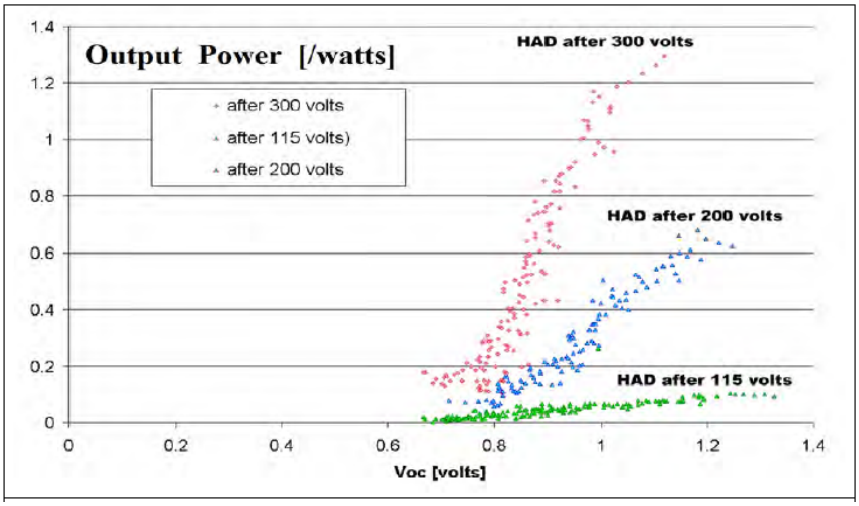

Figure 6. Tardive thermal power as a function of $V_{\rm oc}$ and $V_{\rm applied}$, after disconnection of all input electrical power, for three different experiments (input drive potentials from 115 to 300 V) as a function of $V_{\rm oc}$.

and there appears to be a horizontal component close to the x-axis for some of the curves.

There are three important conclusions. First, $V_{\rm oc}$ alone is NOT predictive of the actual magnitude of the HAD excess enthalpy, as stated above, since there are several HAD-$V_{\rm oc}$ curves. In fact, the observed and expected HAD excess enthalpies based on the linear model is shown in Table 1, and is fairly good above 160 V applied during the active phase.

Second, most importantly, the charging voltage used to drive the system before the HAD plays a major role in the HAD excess enthalpy. In the HAD regime, the HAD enthalpy is controlled by $V_{\rm oc}$ and $V_{\rm applied}$. In each case, the excess enthalpy (HAD) increases with $V_{\rm oc}$.

Third, there is a threshold $V_{\rm oc}$ potential for successful HAD which is ~0.7 V.

4. Interpretation

4.1. The engineering results

4.1.1. *The control of HAD and TTP*

Figure 7 shows the terrific new method used to improve the efficiency by using a duty cycle of <1.0. Figure 7 has eight curves, and four involve power; four involve energy. Shown are the input electrical powers to the Pd/D_2O/Pt system and the control and observed output thermal powers. Also shown are the input and output energies. The input electrical powers and observed output thermal powers are in milliwatts and the energies are in joules, with the values plotted as function of minutes.

To generate Fig. 7, a series of six electrical pulses and rest periods were given, alternately to the ohmic control and the Phusor®-type component. During each pulse $V_{\rm applied}$ was 200 V and the ratio of the active to the rest regime was 1:1, with each pulse width being 1 h. The times of the active drive and the rest periods define the duty cycle. Two representative pulses are labeled. After each active pulse, there is a rest period. when the electrical power source is completely disconnected. Two representative rest times are labeled (“HAD Regime”).

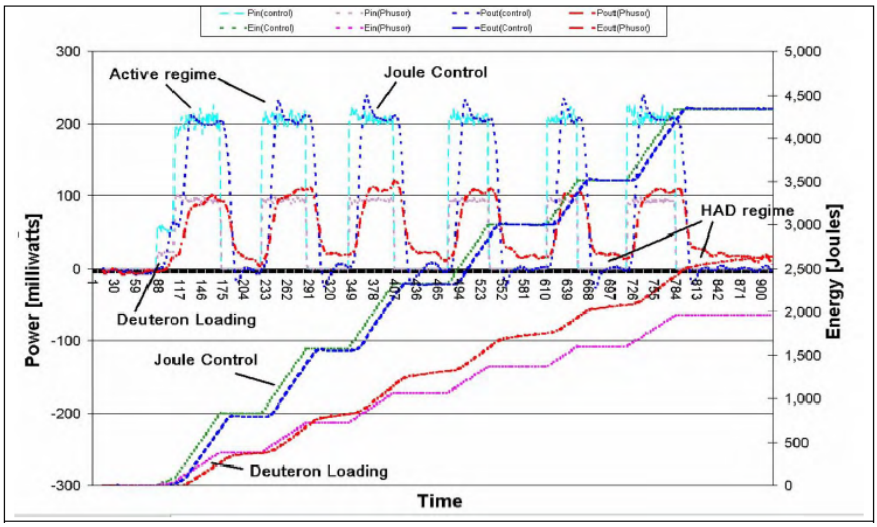

Figure 7. Calorimetry of PHUSOR®-type Pd/D_2O/Pt cell and its joule control‘ as a function of time, with six pulses and a 1:1 duty cycle.

The energy required for loading is small and endothermic, and is accounted for when given off. It is also small compared to the observed excess heat (and the HAD). It can be seen that the observed output power is much greater compared to the electrical input power for the deuteron-loaded Pd/D_2O/Pt device, as compared to the joule control. There is incremental excess power, and tardive thermal power, and net XSH and HAD.

Four additional curves in Fig. 7. also confirm the difference between the control and observed excess heat output of the deuterium-loaded system. They are the integrated energy curves. It can be seen that for the ohmic joule (thermal) control that the integrated energies of the input and output rise with parallel slopes. In contrast, in the deuterium-loaded heavy water systems, there is again the appearance of a gap which increases over time, corroborating that there has been excess heat generated.

Thus, these curves also demonstrate tardive thermal power and HAD. After the devices were driven for several hours, examination of the possible heat after death was made by semiquantitative analysis with correction for a joule (thermal) control, with correction for deloading, with correction for the normal cooling. After accounting for other sources of energy storage and release such as thermal cool-off and deuteron-deloading, it can be seen that HAD does exist and is clearly demonstrated by this apparatus and method.

4.1.2. *Importance of HAD and TTP control*

How important is this new technique? Figure 8 is a bar graph which shows the excess heat gain for a heavy water palladium Phusor®-type Pd/D_2O/Pt system, both during the active phase only, and also the summation of the active phase heat gain with the HAD gain. This set of metrics is shown for three runs, each using one of three different driving voltages. These were applied for two types of duty cycles; the first two runs were 1:1, and the last (300 V applied) was 1:5. In the figure, both the active regime energy gain (front row) and the combined gain using the HAD (back row) are plotted as for the three applied voltages.

Note that there is a significant increase in efficiency when the energy gain including the HAD region is also considered. There is an increase of excess energy 410% beyond that of the active phase alone. Notice also the major

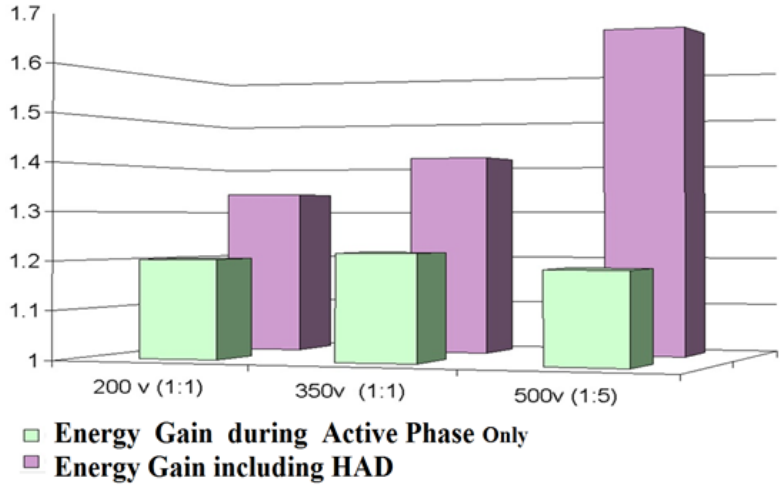

Figure 8. Energy gain in a palladium Phusor®-type Pd/D_2O/Pt system. The front row presents the results during the active phase, alone. The second row presents the results of both the excess energy gain and the semiquantitive HAD enthalpy in the same time period. The duty cycles are discussed in the text.

impact of applied voltage *before* the HAD regime. Thus, Fig. 8 shows the importance of this method for driving CF/LANR cells. This is not trivial in any way.

In fact, a important corollary is that some may have missed observing HAD for a new reason. The failure may have been their failure to look for HAD, or it might mean the absence of all conditions needed for making the active state, or it might indicate that the cells were driven at too low a driving voltage, or they may have had an incorrect indication of CF/LANR (false positive) .

4.1.3. *Lumped component engineering analysis*

To understand these findings about HAD behavior, a lumped component electrical model was used to analyze the HAD excess heat production which continues for several hours after cessation of input electrical power to an active loaded spiral-wound palladium cathode/D_2O/platinum anode system. This resistor – capacitor model allows a rough analysis by separating the flow of deuterons from the charged palladium lattice after cessation of electrical input power into two loss pathways. In the model, these pathways are represented as loss resistors from the loaded (charged palladium lattice) capacitor (Fig. 9). Both V_{applied} and V_{oc} are corrected by the equilibrium threshold potential ($V_{\mathrm{oc,equil}}$), which is 0.7 V.

As shown above, analysis of the several curves which describe the HAD excess enthalpy as a function of V_{oc} (Fig. 6) indicates that the HAD excess enthalpy cannot be directly related to solely V_{oc}. The previously applied voltage has a major role. It appears that the processes might be modeled as follows. In an electrical process, the cold fusion cell can be treated from the anode and cathode ports as a two terminal device [11]. We now analyze the cathode loading itself as a lumped component linear model using a capacitor to represent the deuteron-loaded palladium cathode. This is used for an approximation for several reasons. First, the palladium cathode is actually loaded by the applied electric field. Second, the losses by fusion and deloading offer a rough analysis by separating the two into loss resistors of a loaded (charged) capacitor (Fig. 9).

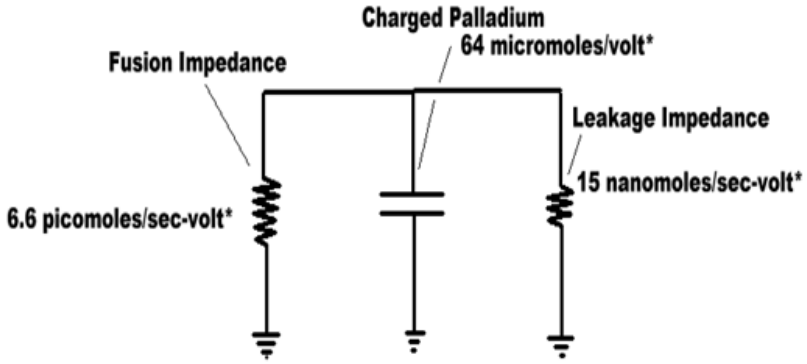

Figure 9. Lumped component linear model of a D-loaded Pd cathode. Shown is the circuit diagram of the simplified lumped component linear model using a capacitor to represent the deuteron-loaded cathode, and the two loss pathways of deuterons from the loaded cathode which are leakage and fusion. The values shown are derived in the text.

Given a cathodic electrode palladium mass, M_{Pd}, palladium's atomic weight of 106.4, the density of the pure palladium metal of 11.97 g/cm^3, and the value of the Avogadro number, then for this electrode with an active volume of ~0.17 cm^3, there are (at most, and probably less when the active number are considered) Q_{Pd} moles of Pd atoms.

$$Q_{\mathrm{Pd}} \sim \mathrm{Vol} \times \rho_{\mathrm{Pd}} \times A_{\mathrm{v}}/M_{\mathrm{w}} = 0.019\ (\mathrm{mol}), \tag{1}$$

$$Q_{\mathrm{Pd}} = 1.15 \times 10^{22}\ \mathrm{Pd\ \ atoms}. \tag{2}$$

For reasons discussed elsewhere [10–12], and for reasons involving the two weeks required for preparation of active cathodes, we can assume there is nearly full loading. Hence, the molar quantity of deuterons is on the order of the number of palladium atoms.

$$Q_{\mathrm{D,Pd}} \sim 0.019\ (\mathrm{mol}). \tag{3}$$

We now consider the univalent deuterons which are generally believed to lose their electron when they enter the palladium metal from the surface as an equivalent charge, and use the Faraday constant, *F*, with the applied voltage analyzed by a linear model. Assume that V_{applied} (300 V to the PHUSOR®-type cell over several weeks of loading) is sufficient to yield a loading of about 1. Then, the proposed linear model based upon the results of this paper (Figs. 6 and 7) suggests that the loading, and HAD, can be handled using a lumped component model using the palladium lattice's deuteron-loading capacitance, and the loss of deuterons to either leakage (most likely) or the desired fusion reactions.

4.1.4. *Pd/D capacitance ($C_{D/Pd}$)*

Using an analogy to capacitors, but corrected from equivalents to moles, we can write the requirement for full loading of the palladium with deuterons (at equilibrium, but which may not occur if the solution electrical conductivity is too high, or if the palladium is cracked, or for any of many other reasons).

The capacitance is determined by the total quantity of deuterons present in the palladium electrode ("concentration"). This is an approximation because complications are that the true proportions which contribute ("activity") may not equal the concentration, and that this is a nonlinear and non-equilibrium system when it is generating excess heat.

$$Q_{\mathrm{D,Pd}} = C_{\mathrm{D,Pd}} * (V_{\mathrm{applied}} - V_{\mathrm{oc,equil}}) = C_{\mathrm{D,Pd}} * (V_{\mathrm{applied}} - 0.7). \tag{4}$$

Here, as elsewhere, V_{applied} is corrected by the observed equilibrium threshold potential ($V_{\mathrm{oc,equil}}$) of 0.7 V*. The superscript star (*) is added to remind the reader than 0.7 V is subtracted.

Since V_{applied} is about 300 V, and $Q_{\mathrm{D,Pd}}$ is about 0.019 mol, then the active palladium lattice can be characterized by a deuteron loading capacitance, $C_{\mathrm{Pd,D}}$, on the order of 64 μml/V*. Again, the star [*] is added to remind the reader that the units used are in volt, but the actual value is semiquantitatively corrected with respect to the equilibrium threshold potential ($V_{\mathrm{oc,equil}}$). This is negligible for the 300 V initially applied, but is especially relevant during the HAD.

$$C_{\mathrm{D,Pd}} = 6.39 \times 10^{-5} (\mathrm{mol/V^*}). \tag{5}$$

4.1.5. *Deuteron HAD fusion current ($I_{\mathbf{HADfusion}}$)*

The initial HAD excess enthalpy is about 1 W. Analysis, and independent measurements, have indicated that helium-4 production is the probable ash of these deuteron-loaded palladium reactions during the active phase [1,2,4].

The same products are probably also produced during the HAD regime, as well. Therefore, for 1 W HAD excess power, there are about 1.2×10^{12} helium nuclei generated per second. Since it takes two deuterons for each reaction, there is a putative fusion current (i.e. deuteron loss) of 2.4×10^{12} deuterons/s, or about 4 pmol/s.

$$I_{\mathrm{HADfusion}} = 3.98 \times 10^{-12} (\mathrm{mol/s}). \tag{6}$$

4.1.6. *Admittance for fusion reactions, $Y_{\mathbf{fusion,Pd,D}}$*

In the lumped component model, during the HAD regime, the HAD fusion current, $I_{\mathrm{HADfusion}}$, is the product of an admittance and the electric potential available (equal to the open circuit voltage minus the equilibrium threshold potential ($V_{\mathrm{oc,equil}}$)).

$$I_{\mathrm{HADfusion}} = Y_{\mathrm{fusion,Pd,D}} * (V_{\mathrm{oc}} - 0.7) (\mathrm{mol/s}), \tag{7}$$

$$Y_{\mathrm{fusion,Pd,D}} = 6.64 \times 10^{-12} (\mathrm{mol/s\text{-}V^*}). \tag{8}$$

$Y_{\mathrm{fusion,Pd,D}}$ is linear approximation of the loss of deuterons to the desired fusion reactions. $Y_{\mathrm{fusion,Pd,D}}$ is thus the functional admittance for the HAD fusion reactions, and is about 6.6 pmol/s-V*. The star [*] is again added to remind the reader that the units used are in volt, but the value is semiquantitatively corrected with respect to the equilibrium threshold potential ($V_{\mathrm{oc,equil}}$). This is especially important relevant during the time of the HAD.

4.1.7. *Analysis of admittance for leakage ($Y_{leakage}$)*

It is the inevitable loss of deuterons by leakage from the loaded palladium lattice that ultimately terminates the desired HAD reactions. The lumped component values representing deuteron-leakage can be determined from the washout of the HAD excess power. Consideration of the RC time constant of 70 min (4200 s) can be used to determine the loss resistance representing deuteron leakage.

It is reasonable to assume that deuteron loss by leakage is much greater than deuteron loss by the desired reactions, and this will be checked to confirm that the deuteron leakage resistance is much smaller than the deuteron fusion resistance, after deriving the leakage resistance. The fusion resistance is determined from the fusion admittance by an inverse function. By circuit analogy, the $Y_{\mathrm{fusion,Pd,D}}$ has an equivalent HAD fusion resistance of 1.5×10^{11} (s-V*/mol).

$$Y_{\mathrm{fusion,Pd,D}} = 1/R_{\mathrm{fusionPd,D}}(\text{mol/(s-V*)}), \tag{9}$$

$$R_{\mathrm{fusionPd,D}} = 1.5 \times 10^{11}(\text{s-V*/mol}). \tag{10}$$

The leakage resistance is derived using the lumped component model (see Fig. 9), where the model correctly includes the losses of deuterons to both leakage and fusion. Here, for an approximation the fusion resistance is assumed to be infinite for this calculation.

Therefore, because $C_{\mathrm{D,Pd}} = 6.39 \times 10^{-5}$ mol/V*, then the solution can be found because the time constant, τ, is RC.

$$\tau = 4200\text{s} \cong R_{\mathrm{Leakage}} * C_{\mathrm{D,Pd}} = R_{\mathrm{Leakage}}(\text{s-V*/mol})\ 6.39 \times 10^{-5}(\text{mol/V*}). \tag{11}$$

Thus, R_{Leakage} is derived to be about 6.57×10^7 s-V*/mol. Inverting this deuteron leakage resistance from actual deloading results in the deuteron loss admittance.

$$R_{\mathrm{Leakage}} = 6.57 \times 10^7(\text{s-V*/mol}), \tag{12}$$

$$Y_{\mathrm{Leakage}} = 1.52 \times 10^{-8}(\text{mol/(s-V*)}). \tag{13}$$

This value of deuteron leakage admittance must be compared to the HAD fusion admittance. Using this lumped component model, the ratio of the two admittances determines the efficiency of the desired HAD excess enthalpy reactions.

The experiments here suggest that initially only one in 2300 deuterons takes part in the desired reactions of HAD excess enthalpy production, for a net utilization of 0.04% of the loaded deuterons at that time. This decreases over time. Integrated over the entire HAD regime, this deuteron participation levels falls, and eventually only 1 in 10^6 deuterons participates in the desired fusion reactions.

The small number of the ratio is consistent with the fact that the desired reactions are infrequent to very rare. The small number is also consistent with the approximation used to derive these values.

5. Conclusions

5.1. Comparison of model with observation

In the HAD regime, the excess enthalpy appears to be controlled by V_{oc}, V_{applied}, and the capacitance of the cathode ($\sim 64\mu$mol/V*). The form factor might be similar to that for other electrical engineering systems such that $E_{\mathrm{HADfusion}}$

is related to Q_{Pd}, V_{applied}, and V_{oc}. $E_{\mathrm{HADfusion}}$ is the energy in the filled lattice availed for, and delivered to, fusion in the HAD regime. Given the capacitance of the palladium lattice ($C_{\mathrm{Pd,D}}$), then the total quantity of deuterons available for fusion within the loaded palladium (Q_{Pd}) is determined from V_{applied}, and $E_{\mathrm{HADfusion}}$ is determined by both V_{applied} and V_{oc}.

$$Q_{\mathrm{Pd}} = (C_{\mathrm{Pd,D}}\, V_{\mathrm{applied}}), \tag{14}$$

$$E_{\mathrm{HADfusion}} = Q_{\mathrm{Pd}}\, V_{\mathrm{oc}} = (C_{\mathrm{Pd,D}}\, V_{\mathrm{applied}})\, V_{\mathrm{oc}}. \tag{15}$$

Plugging in measured and derived values for the three cases, and correcting by the Faraday, F, to correct for the use of Farads and volts, yields the results of Table 1. In the table, it can be seen that the values expected, generated by the model (E), are in the general range expected compared with the observed values of HAD excess enthalpy (O).

This fairly good correlation is encouraging. In fact, if the actual V_{oc} had been used instead of the 1 min average, then the correlations might have been more accurate, because the expected values would have increased, consistent with the higher electrical drive levels.

5.2. Final implications and summary

There remain some very important results and implications of these TTP measurements. First, TTP is apparent in palladium in heavy water driven in active excess heat-producing cold fusion systems. This is very important because the energy gain can be increased by at least 410%.

Second, the advantages of studying TTP are many. Most importantly, there is no interfering input electrical power and resultant, and inexorably associated, noise. Examination of TTP provides improved understanding of cold fusion reaction kinetics, as well as where the desired reactions occur and what are their magnitudes. However, good engineering requires that TTP voltages be redefined with respect to removing 0.7 V to make them more useful as an engineering quantity. The experiments here measured the active palladium lattice's HAD deuteron-loading capacitance which is 64 μ mol/V*. The admittance for the desired excess enthalpy HAD reactions ($Y_{\mathrm{fusion,Pd,D}}$) is 6.6 pmol/(s-V*). That admittance is dwarfed by the system's deloading loss admittance (Y_{Leakage}) which is 15 nmol/(s-V*). This is what causes the deloading and penultimate loss of the HAD excess enthalpy.

Third, the experiments here revealed that initially only one in 2300 deuterons takes part in the desired reactions of HAD excess enthalpy production, for a net utilization of 0.04% of the loaded deuterons at that time. This decreases over time. Importantly, integrated over the entire HAD regime, this deuteron participation levels falls, and eventually only 1 in 10^6 deuterons participates in the desired fusion reactions.

There are several important implications for scientific experiments and commerce. One implication of the presence of heat after death is that complete sample characterization requires more than simply the knowledge of the power gain and the optimal operating point ("peak production") curves. Full and proper sample characterization requires measuring not only the driving manifold (which elicits knowledge of the optimal operating point) but also the changes of the sample which actually is producing TTP.

Second, another implication of this study of heat after death is that the use of a simple power gain factor to characterize a device is incomplete. It might be several times greater.

Third, these discoveries are an important group of findings because the error in measuring heat after death might be quite high, as well. This is especially true if one does not take into account the impact of duty cycle, and the previously applied electrical potential during the active state, and other issues such as HAD-region enhancing and quenching materials.

Fourth, as a corollary, others may be reporting lower limit of what is actually achieved in terms of their samples' performances. Simply put, the excess heat ("XSH") generated by an active conventional aqueous cold fusion system may be at their lower limits. The corrected sample activity is actually obtained only when using a calibrated active device which has been properly loaded, and run with the full consideration of the HAD excess enthalpy.

Fifth, there are implications involving the HAD and outgassing from proton- and deuteron-loaded metal, and the roles of gold (Swartz) and boron (Miles) and mercury (McKubre, Tanzella) must be reconsidered. Materials which control deloading are critical.

In summary, these measurements of HAD excess enthalpy, the roles of $V_{\rm oc}$ and $V_{\rm applied}$ in that excess heat, and the existence of the equilibrium threshold potential ($V_{\rm oc,equil}$), herald improved ways of both characterizing and operating deuteron-loaded palladium cathodes. Therefore, the optimization of cold fusion devices has a new dimension. Due to magnitude of the parameters involved during the HAD regime, it must be considered and factored in for optimization of any sample's true over-unity performance. Engineered-TTP [27] clearly can make some cold fusion devices and systems more efficient.

Acknowledgments

The author acknowledges and thanks Gayle Verner for her experimental and editorial assistance, and Prof. David Nagel for his significant suggestions and comments. This effort was supported by JET Energy Inc. and the New Energy Foundation. PHUSOR® is a registered trademark. PHUSOR® -technology and some of the other technologies described here are protected by patents pending.

References

[1] M. Swartz, Survey of the observed excess energy and emissions in lattice assisted nuclear reactions, *J. Scientific Exploration* **23**(4) (2009). 419–436.

[2] C. Beaudette, *Excess Heat & Why Cold Fusion Research Prevailed*, Second Edition, ISBN 9-9678548-2-2 (2002).

[3] M. Swartz, Codeposition of palladium and deuterium, *Fusion Technol*. **32** (1997) 126–130.

[4] M.H. Miles, *Thermal and Nuclear Aspects of the Pd/D_2O Systems*, Volume 1: A Decade of Research at Navy Laboratories, S. Szpak and P.A. Mosier-Boss (Eds.), Technical Report 1862, SSC San Diego (February 2002).

[5] S. Pons and M. Fleischmann, *Heat After Death, Proc. ICCF4*, Lahaina, Maui, Dec. 6–9, 1993. EPRI TR104188-V2, Vol. 2 : p. 8-1 (1994); and *Trans. Fusion Technol*. **26** (4T), Part 2, (December 1994) 87.

[6] M.H. Miles, S. Szpak, P.A. Mosier-Boss and M. Fleischmann, Thermal behavior of polarized Pd/D electrodes prepared by codeposition, *The Ninth Int. Conf. on Cold Fusion* (2002).

[7] M.H. Miles, M. Fleischmann and M.A. Imam, Calorimetric analysis of a heavy water electrolysis experiment using a Pd-B alloy cathode, Naval Research Laboratory Report NRL/MR/6320-01-8526, 155 pp. (March 16, 2001).

[8] Mizuno, Tadahiko "Nuclear Transmutation: The Reality of Cold Fusion", Infinite Energy Press Concord, New Hampshire, (1998)

[9] M. Swartz and G. Verner, Dual Ohmic Controls Improve Understanding of "Heat after Death", *Trans American Nuclear Soc*., vol. 93, ISSN:0003-018X, 891-892 (2005).

[10] M. Swartz and G. Verner, Two site of cold fusion reactions viewed by their evanescent tardive thermal power, Abstract ICCF-11 (2004).

[11] M. Swartz, Kinetics and lumped parameter model of excess tardive thermal power, Mitchell Swartz, APS (2005).

[12] M. Swartz, Spatial and temporal resolution of three sites characterizing lattice-assisted nuclear reactions, APS 2008; M. Swartz, Colloquium on LANR in Deuterated Metals Colloquium on LANR at MIT, August 2007.

[13] M. Swartz, Consistency of the biphasic nature of excess enthalpy in solid state anomalous phenomena with the quasi-1-dimensional model of isotope loading into a material, *Fusion Technol*. **31** (1997) 63–74.

[14] M. Swartz and G. Verner, Excess heat from low electrical conductivity heavy water spiral-wound Pd/D_2O/Pt and Pd/D_2O–$PdCl_2$/Pt devices, Condensed Matter Nuclear Science, *Proc. ICCF-10*, Peter L. Hagelstein and Scott, R. Chubb (Eds.), World Scientific, NJ, ISBN 981-256-564-6, 29-44 (2006).
[15] M. Swartz, Can a Pd/D_2O/Pt device be made portable to demonstrate the optimal operating point? *ICCF-10* (Cambridge, MA), 2003.
[16] M. Swartz and G. Verner, Photoinduced excess heat from laser-irradiated electrically-polarized palladium cathodes in D_2O, Condensed Matter Nuclear Science, *Proc. ICCF-10*, ISBN 981-256-564-6, 213-226 (2006).
[17] M. Swartz, Improved electrolytic reactor performance using OOP system operation and gold anode, *Trans. Amer. Nucl. Assoc*., Nashville **78** (1998) 84–85. Meeting, (ISSN:0003-018X publisher LaGrange, Ill).
[18] M. Swartz and G. Verner, The Phusor®-type LANR cathode is a metamaterial creating deuteron flux for excess power gain, *Proc. ICCF14* 2, (2008), p 458; ISBN: 978-0-578-06694-3, 458, (2010); www.iscmns.org/iccf14/ProcICCF14b.pdf.
[19] M. Swartz, Excess power gain using high impedance and codepositional LANR devices monitored by calorimetry, heat flow, and paired stirling engines, *Proc. ICCF14* 1, (2008), p 123; ISBN: 978-0-578-06694-3, 123, (2010); www.iscmns.org/iccf14/ProcICCF14a.pdf.
[20] M. Swartz, Metamaterial shaped LANR-cathodes produce deuteron flux, *Infinite Energy* **90** (2010).
[21] M. Swartz, Optimal operating point manifolds in active, loaded palladium linked to three distinct physical regions, *Proc. ICCF14* 2, (2008), p 639; ISBN: 978-0-578-06694-3, 639, (2010); www.iscmns.org/iccf14/ProcICCF14b.pdf
[22] M. Swartz, Optimal operating point characteristics of nickel light water experiments, *Proc. ICCF-7*, 1998.
[23] M. Swartz, Control of low energy nuclear systems through loading and optimal operating points, ANS/2000 Int. Winter Meeting, Nov. 12–17, 2000, Washington, D.C. (2000).
[24] M. Swartz, Three Physical regions of anomalous activity in deuterided palladium, *Infinite Energy* **14**(61) (2008) 19–31.
[25] D. Nagel, ICCF13, Sochi, Russia, Powers, Materials and radiations from low energy nuclear reactions on surfaces (2007).
[26] M.R. Swartz, Excess heat and electrical characteristics of type “B” anode-plate high impedance Phusor-type LANR devices, American Chemical Society, Salt Lake City, UT, *J. Sci. Exploration* **23** (4) (2009)491–495.